

Influence of Working Lining Parameters on Temperature and Stress Field of Ladle

Gongfa Li¹, Peixin Qu², Jianyi Kong^{1*}, Guozhang Jiang¹, Liangxi Xie¹, Zehao Wu¹, Po Gao¹, Yuan He¹

¹College of Machinery and Automation, Wuhan University of Science and Technology, Wuhan 430081, China

²School of Information Engineering, Henan Institute of Science and Technology, Xinxiang 453003, China

Received: 17 Sep. 2012; Revised 21 Nov. 2012; Accepted 22 Nov. 2012

Published online: 1 Mar. 2013

Abstract: Ladle is an important apparatus in metallurgical industry and takes charge of transferring molten steel from a converter to procedure of continuous casting or ingot casting. It not only improves production efficiency, product quality and production flexibility massively, but also decreases energy and material consumption. The ladle lifetime influences economic benefit of iron and steel enterprises directly. Distribution of its temperature field and stress field has a vital effect on the lifetime. Thermal expansion stress is one of important reasons for damage as ladles operate under the condition of high temperature and overload. Under high temperature, thermal expansion is generated in the ladle lining and shell. Thermal expansion stress is introduced when lining and shell deformation arising from thermal expansion is subjected to mutual constraint from the counterpart due to various thermal expansion coefficient. The finite element software is used to establish the ladle model and influence of working lining material thermal conductivity; thermal expansion coefficient, Young's modulus and its thickness on the ladle temperature and stress field are studied. The calculation result indicated the equivalent stress in the ladle enlarged as the thermal conductivity, thermal expansion coefficient, Young's modulus of working-lining material increased and the thickness decreased. Research in this paper plays a referring role in comprehending distribution of temperature field and stress field of the ladle and selecting appropriately physical parameters of lining. The actual operation result indicates that the research increases the ladle lifetime effectively and shows its wide popularization value.

Keywords: Ladle composite construction body, Work lining, Physical parameter, Thickness, Temperature field, Stress field, Finite element method

1. Introduction

Ladle is an important vessel in the metallurgical industry. It acts in storing and transferring molten steel and its service life directly affects the normal production and cost of corporations. When the ladle is put into service, its lining temperature distribution has a vital effect on the lining thermo mechanical stress distribution, even service life. [1],[2] Thus, it is necessary to comprehend the ladle temperature and stress distribution.

Research of the ladle temperature and stress deepens continuously with the development of refractory material and advance of steel-making process. Its main purpose is to analyze reasons of the shell temperature increase, refractory material erosion and structure instability as well as to look for measures [3]. G.S.Sarmiento [4] developed software TEMPCU specialized in analysis of the ladle tem-

perature field and stress field. The software adopted the finite element method to establish two dimensional model of the ladle. The temperature field and stress field could be analyzed in all stages of ladle preheating, Subjected steel, refining and conveyance, pouring as well as cooling; J.Y Kong [5] researched influence of the ladle working lining thickness and heat transfer coefficient on its temperature; G.Z Jiang [6] researched the influence of refractory material physical parameters and various working lining thickness on distribution of stress field of ladle wall during the process of receiving steel and offered some references for the ladle design; Z.G Wang [7] used the finite element method to implement numerical simulation on ladle bottom temperature and stress field. The calculation result indicated that the ladle is still in the state of absorbing heat after preheating and reached to "quasi-steady state" after several heat recycles; After preheating, stress value of

* Corresponding author: e-mail: jykong_1961@yahoo.com.cn

working layer of the ladle bottom reached to the maximum at the instance of pouring molten steel; stress in the ladle bottom working layer hot surface near to the ladle wall is higher than that near to the center. The insulated device is installed near to the ladle wall to diminish its stress.

From above, it can be seen from research of the ladle in foreign nations and domestic that their research mainly focus on control of ladle temperature and influence of various lining material on ladle temperature and stress distribution.

2. Temperature and Stress of Ladle

The calculation process of thermal stress of the ladle [8] is commonly divided into procedures as follows: deformation under the condition of given constraint is calculated according to the ladle temperature distribution and thermal expansion coefficient at every section of the ladle. And then the geometric equation is applied to computing strain at each point within the ladle in the light of deformation displacement. Finally, stress at each point within the ladle is calculated by strain in accordance with the ladle material physical equation (relation between stress and strain).

1. Geometric equation of stress field of the ladle-strain-displacement relation

It is in matrix form represented as following.

$$\varepsilon = \begin{bmatrix} \frac{\partial}{\partial x} & 0 & 0 \\ 0 & \frac{\partial}{\partial y} & 0 \\ 0 & 0 & \frac{\partial}{\partial z} \\ \frac{\partial}{\partial y} & \frac{\partial}{\partial x} & 0 \\ 0 & \frac{\partial}{\partial z} & \frac{\partial}{\partial y} \\ \frac{\partial}{\partial z} & 0 & \frac{\partial}{\partial x} \end{bmatrix} v \quad (1)$$

Where $\varepsilon = [\varepsilon_x, \varepsilon_y, \varepsilon_z, \gamma_{xy}, \gamma_{yz}, \gamma_{xz}]^T$ denotes strain at each point within the ladle. $v = [u, v, w]^T$, u, v, w denote displacement along the direction of x, y and z , respectively. Stress at each point within the ladle is calculated by the ladle physical equation according to strain above. And force which the ladle is subjected to conforms to the equilibrium equation.

2. Physical equation of stress field of the ladle-strain-stress relation

The generalized Hook's law is applied to representing it as:

$$\sigma = \frac{E(1-\nu)}{(1+\nu)(1+2\nu)} \times \begin{bmatrix} 1 & \frac{\nu}{1-\nu} & \frac{\nu}{1-\nu} & 0 & 0 & 0 \\ \frac{\nu}{1-\nu} & 1 & \frac{\nu}{1-\nu} & 0 & 0 & 0 \\ \frac{\nu}{1-\nu} & \frac{\nu}{1-\nu} & 1 & 0 & 0 & 0 \\ 0 & 0 & 0 & \frac{1-2\nu}{2(1-\nu)} & 0 & 0 \\ 0 & 0 & 0 & 0 & \frac{1-2\nu}{2(1-\nu)} & 0 \\ 0 & 0 & 0 & 0 & 0 & \frac{1-2\nu}{2(1-\nu)} \end{bmatrix} \varepsilon \quad (2)$$

Where E is Young's modulus, ν is Poisson's ratio.

3. Equilibrium equation of the Ladle

For the three dimensional problem, Equilibrium equation at each point along the direction of coordinate x, y and z within the ladle is:

$$\begin{aligned} \frac{\partial \sigma_x}{\partial x} + \frac{\partial \tau_{yx}}{\partial y} + \frac{\partial \tau_{zx}}{\partial z} + f_x &= 0 \\ \frac{\partial \tau_{xy}}{\partial x} + \frac{\partial \sigma_y}{\partial y} + \frac{\partial \tau_{zy}}{\partial z} + f_y &= 0 \\ \frac{\partial \tau_{xz}}{\partial x} + \frac{\partial \tau_{yz}}{\partial y} + \frac{\partial \sigma_z}{\partial z} + f_z &= 0 \end{aligned} \quad (3)$$

Where f_x, f_y and f_z are volume force of the ladle unite volume at the direction of x, y and z .

4. Temperature and Stress of the Ladle

The American scholar Millet L Wei derives calculation formulae of the single-layer method which are utilized to calculate the ladle temperature stress [9]. The calculation principle of the single-layer method is to regard refractory material as a single-layer loop and esteem the ladle loop as another loop. At the same time, the method adopts an experience parameter-equivalent clearance which denotes initial looseness or slot in the radial and circumferential direction between refractory bricks and meanwhile revises the simplified manner during establishing the model and adjusts unsteady situations of refractory material under the condition of high temperature. Fig.1 denotes the calculation diagram of the single-layer method.

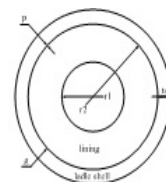


Figure 1 Calculation diagram of the single-layer method.

Equivalent clearance parameter is regarded as a function about the radius of the interface between lining and the ladle shell. Coefficient in the function expression is ascertained according to experience as well as analysis and research work. During preheating the ladle, lining expansion makes the ladle shell generate stress. Moreover, the shell maximum stress value arises during the period. The shell maximum stress value is calculated according to equation (4).

$$\sigma_s = \frac{pr_2}{t_s} \quad (4)$$

Refractory brick stress is computed according to equation (5).

$$\sigma_b = \frac{-2pr_2^2}{r_2^2 - r_1^2} \quad (5)$$

Interaction press is calculated according to equation (6).

$$P = \frac{C}{A+B} \tag{6}$$

Here:

$$A = \frac{r_2}{E_b} \left(\frac{r_2^2 + r_1^2}{r_2^2 - r_1^2} - \nu_b \right)$$

$$B = \frac{r_2}{E_s} \left(\frac{r_2}{t_s} + \nu_s \right)$$

$$C = \frac{1}{2\alpha_b \Delta T_b (r_1 + r_2)} - \alpha_s \Delta T_s r_2 - g$$

P is interaction force between lining bricks and the ladle shell, α_s, α_b are the ladle shell and lining brick stress caused by expansion, respectively, τ_1, τ_2 are the lining inner and outer radius, respectively, t_s is ladle shell thickness, α_s, α_b are thermal expansion coefficient of the ladle shell and lining brick, respectively, $\Delta T_s, \Delta T_b$ are temperature increment of the ladle shell and lining brick, respectively, E_s, E_b are Young's modulus of the ladle shell and lining brick, respectively, ν_s, ν_b are Poisson's ratio of the ladle shell and lining brick, respectively, g is experience's equivalent clearance of the ladle shell, and the selected interface radius is 0.075%.

3. Two-dimensional model of ladle

As both the ladle structure and supported load are symmetric about the axis of the ladle, any revolving cross section in the ladle was defined as the finite element analysis object. The model was simplified without influencing results of the temperature field and stress field in the ladle composite construction body. Its revolving cross section was shown in Fig.2.

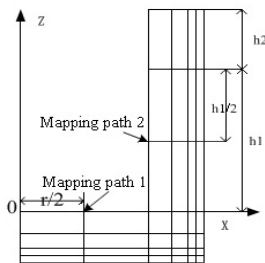


Figure 2 Revolving cross section of the ladle.

The slag-line layer was composed of magnesia-carbon bricks and the rest of the working lining on the wall and on the bottom selected alumina-magnesia-carbon. The first and second permanent layers on the wall and bottom were

constructed with high alumina bricks. Physical properties of the magnesia-carbon brick, high alumina brick, alumina-magnesia-carbon brick, and steel shell were referred to the literature [8].

When the finite element method was utilized into the analysis, boundary conditions were commonly dealt with according to two kinds: one was that the inside surface of the ladle lining was specified at 1650°C the other was that heat-exchanging conditions of the outside of the ladle shell, which were calculated in accordance with the literature [9], were obtained by experiment, and then heat-exchanging conditions got an essential modification depending on measured results of temperature of the outside surface of the ladle shell, in order to make the obtained analysis model present the actual working condition.

According to the model above, physical parameters and boundary conditions, temperature distribution of the ladle was calculated and then the temperature as a form of a body load was loaded on the model to fulfill the thermal-stress calculation. In order to determine laws of temperature and stress distribution of the ladle bottom along the axis and the wall along the radius direction, the equivalent stress was mapped onto two typical paths selected in Fig.1 by the function of mapping results onto a path in the FEA software.

4. Physical parameters of working lining Influencing the temperature and stress field

Physical parameters referring to calculation of the stress field incorporates density, heat capacity, thermal conductivity, Young's modulus and Poisson's ratio. However, it is generally viewed that both density and Poisson ratio are independent of temperature. That is, four physical properties for one material have an effect on the stress field distribution. As materials in ladle-bottom localized regions (such as the porous brick, nozzle brick and shock block) are little geometrical proportion, they just affect the temperature field and stress field in their surrounding adjacent regions. Whereas, they are negligible, with respect to little affecting the stress field of the entire ladle sufficiently. Thus, the entire ladle only involves four materials. Working lining's Alumina-magnesia-carbon material in the ladle bottom and wall, high alumina brick material of the permanent lining, magnesia-carbon material of slag line bricks on the ladle wall and metal material of the ladle shell are considered, namely. Thus parameters affecting the stress field in the overall ladle reach up to sixteen. Moreover, the change in each physical parameter affects other physical parameters. Hence, it is unrealistic to make them clear in sequence.

Computing temperature distribution and stress distribution in the ladle lining, we consider the effect of its physical change on the stress field regardless of the change in other physical properties. In general, the thermal conductivity, thermal expansion coefficient and Young's modulus of materials have a greater effect on the stress field.

In addition, the temperature field and stress field are also somewhat determined by the ladle structure, such as working layer thickness, lining expansion joint, whether heat insulating layer was applied, and outer shell shape, attachment structure (trunnion, ladle base, saddle, and counterweight plate). In this paper, the effect of its working lining physical parameters and thickness on them was only taken into account without regard to affecting of the lining expansion joint on them which was referred to the literature [10].

In this paper, any revolving cross section was chosen as the research object to analyze effects of the thermal conductivity, thermal conductivity coefficient and Young's modulus on the stress field in the ladle respectively. And the ladle temperature and stress field under the operating condition of the ladle cast steel were calculated with the same boundary condition.

4.1. Thermal Conductivity Influencing Ladle Temperature and Stress Field

When thermal conductivity value of ladle working lining material, under the condition of confirming the ladle shell temperature less than 420°C , was altered from original $1.15 \text{ W}(\text{mgK})^{-1}$ to $0.5 \text{ W}(\text{mgK})^{-1}$, $2 \text{ W}(\text{mgK})^{-1}$ and $3 \text{ W}(\text{mgK})^{-1}$, respectively, it was obtained through analysis and calculation that the equivalent stress contour along the mapping path 1 (on the ladle wall) and mapping path 2 (on the ladle wall) was shown in Fig.3-Fig.6. From Fig.3-Fig.6, on the basis of other conditions kept, thermal conductivity value of ladle working lining material expanded from $0.5 \text{ W}(\text{mgK})^{-1}$ into $3 \text{ W}(\text{mgK})^{-1}$. Temperature change along the mapping path 1 and 2 is uniform basically. Temperature at the same point of mapping paths arises as thermal conductivity increases. The lowest temperature along the mapping path 1 rises from 176.8°C to 299.4°C , and the lowest temperature along the mapping path 2 rises from 241.8°C to 409.8°C . The equivalent

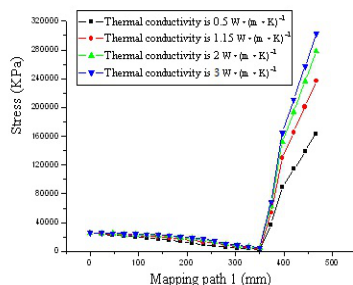


Figure 3 Equivalent temperature contour along mapping path 1.

stress along the mapping path 1 reached to the minimum

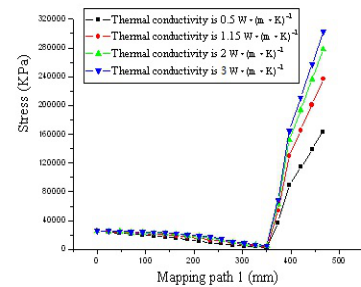


Figure 4 Equivalent stress contour along mapping path 1.

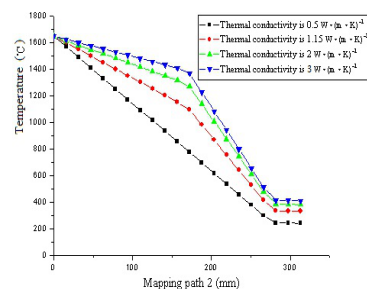


Figure 5 Equivalent temperature along mapping path 2.

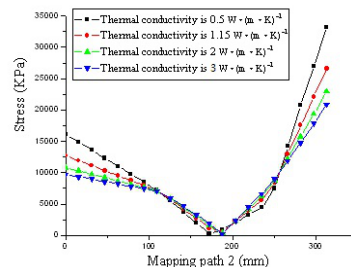


Figure 6 Equivalent stress along mapping path 2.

value of 0MPa at 350mm (The thermal layer was considered as a starting point). The equivalent stress between 0mm and 350mm varied a little with the thermal conductivity, whose value ranged from 0MPa to 25.7MPa; the equivalent stress between 350mm and 467mm was proportional to both the thermal conductivity and the distance, whose value ranged from 0MPa to 302.6MPa. Along the mapping path 2, the minimum stress 0MPa was located between 170mm and 195mm (the thermal layer of the working lining was considered as a starting point), whose location moved towards the ladle outer shell as the thermal conductivity increased. The equivalent stress between 0mm and 110mm decreased as both the thermal conductivity and distance expanded, whose value varied from 7.2MPa to 16.1MPa; the equivalent stress between 110mm and 260mm

did not vary great with conductivity, whose value varied from 0MPa to 14.2MPa; the equivalent stress between 260mm and 313mm, whose value varied from 14.2MPa to 302.6MPa, decreased as the thermal conductivity expanded, but it was proportional to distance.

For other conditions being kept invariable, note that temperature at the same location(except the thermal layer of the working layer) of the ladle increased as thermal conductivity of working lining material of the ladle expanded; the equivalent stress at the same location of the ladle bottom also increased as the thermal conductivity expanded, whose increment decreased earlier but expanded later; the equivalent stress at the same location of the ladle wall declined mainly as the thermal conductivity expanded, whose distribution presented a wave-trough shape in the overall interval.

4.2. Thermal Expansion Coefficient Influencing Ladle Stress Field

As thermal expansion coefficient of working lining material of the ladle was altered from original $8.5 \times 10^{-6} K^{-1}$ into $2.8 \times 10^{-6} K^{-1}$, $5.6 \times 10^{-6} K^{-1}$ and $11.2 \times 10^{-6} K^{-1}$, respectively, by analysis and calculation the stress contours along the mapping path 1 and 2 were obtained, which were shown in Fig.7 and Fig.8, respectively. From Fig.7

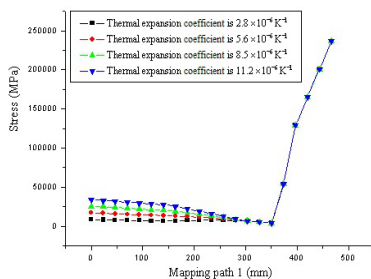


Figure 7 Equivalent stress along mapping path 1.

and Fig.8, note that on the basis of other conditions kept, thermal expansion coefficient of working lining material of the ladle expanded from $2.8 \times 10^{-6} K^{-1}$ into $11.2 \times 10^{-6} K^{-1}$. The equivalent stress along the mapping path 1 increased between 0mm and 350mm as thermal expansion coefficient was augmented, whose value belonged to the interval between 0MPa and 34.3MPa and whose increment declined as distance increased; the equivalent stress between 350mm and 467mm was independent of thermal expansion coefficient, whose value was within the interval between 0MPa and 236.8MPa. The equivalent stress along the mapping path 2 increased between 0mm and 175mm as thermal expansion coefficient was augmented, whose value belonged to the interval between 0.8MPa and

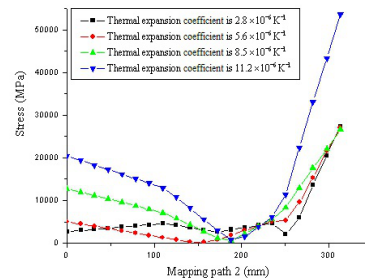


Figure 8 Equivalent stress along mapping path 2.

20.4MPa and whose increment declined as distance increased; the equivalent stress between 175mm and 220mm declined as thermal expansion coefficient expanded, whose value was within the interval between 0MPa and 4.1MPa; the equivalent stress between 220mm and 313mm expanded as thermal expansion coefficient increased, whose value was within the interval between 2.2MPa and 53.6MPa and whose increment was expanded as distance increased.

On the basis of other conditions kept, note that the equivalent stress at the same location of the ladle bottom increased between 0mm and 350mm as thermal expansion coefficient of working lining material of the ladle was augmented. The equivalent stress between 350mm and 467mm was kept invariable; the equivalent stress at the same location of the ladle wall was presented as a wave-trough shape, which increased in two ends but declined in the middle as thermal expansion coefficient enlarged.

4.3. Young's Modulus Influencing Ladle Stress Field

As Young's modulus of working lining material of the ladle was altered from the original 6.3GPa into 4GPa, 8GPa, and 10GPa, respectively, through analysis and calculation stress contours along the mapping path 1 and 2 were obtained, which were shown in Fig.9 and Fig.10, respectively.

From Fig.9 and Fig.10, note that as Young's modulus of working lining material of the ladle expanded from 4GPa into 10GPa on the basis of other conditions kept, the equivalent stress along the mapping path 1 increased between 0mm and 350mm as Young's modulus was augmented, whose value belonged to the interval between 0MPa and 40.8MPa and whose increment declined as distance increased; the equivalent stress between 350mm and 467mm was independent of Young's modulus, whose value was within the interval between 0MPa and 236.9MPa.

The equivalent stress along the mapping path 2 increased between 0mm and 170mm as Young's modulus was augmented, whose value belonged to the interval between 0.8MPa and 19.2MPa and whose increment declined as distance increased; the equivalent stress between 170mm and 220mm was independent of thermal expansion coefficient, whose

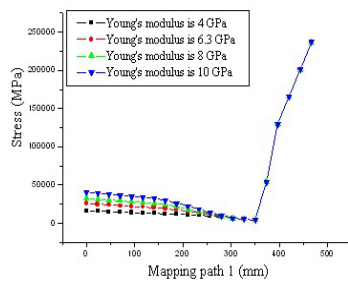


Figure 9 Equivalent stress along mapping path 1.

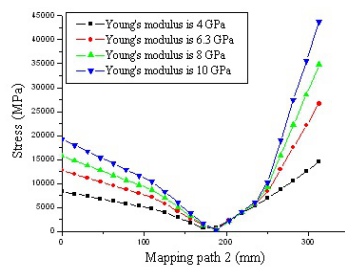


Figure 10 Equivalent stress along mapping path 2.

value was within the interval between 0MPa and 3.8MPa; the equivalent stress expanded between 220mm and 313mm as Young's modulus increased, whose value pertained to the interval between 3.8MPa and 43.7MPa and whose increment enlarged as distance was augmented.

For other conditions kept, note that the equivalent stress at the same location of the ladle bottom increased between 0mm and 350mm as Young's modulus of working lining material of the ladle enlarged. The equivalent stress between 350mm and 467mm was kept invariable; the equivalent stress at the same location of the ladle wall was labeled as a trough shape, which increased in two ends but declined in the middle as Young's modulus enlarged.

4.4. Application Scope of Physical Parameters in the Working Lining

From three above sections about laws of effect of working-lining physical parameters on the ladle stress field, note that 16MnR alloy steel was selected for the ladle outer shell and alumina-magnesia-carbon material was chosen for the working lining. The following discussed application scopes of physical parameters of the working lining made of alumina-magnesia-carbon material based on such extreme conditions as the ladle outer shell temperature less than creep temperature 400°C of 16MnR alloy steel and crushing strength 56.2MPa of alumina-magnesia-carbon bricks.

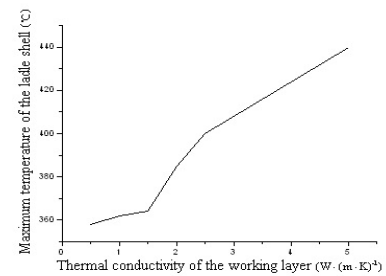


Figure 11 Maximum temperature variation of the ladle outer shell.

Fig.11 gave the maximum temperature profile of the ladle outer shell on the basis of thermal conductivity of the working lining made of alumina-magnesia-carbon material expanded from $0.5 \text{ Wg}(\text{mgK})^{-1}$ into $5 \text{ Wg}(\text{mgK})^{-1}$. Note that thermal conductivity of the working lining made of alumina-magnesia-carbon material was less than $2.5 \text{ Wg}(\text{mgK})^{-1}$ as to the ladle outer shell temperature within creep temperature 400 °C of 16MnR alloy steel.

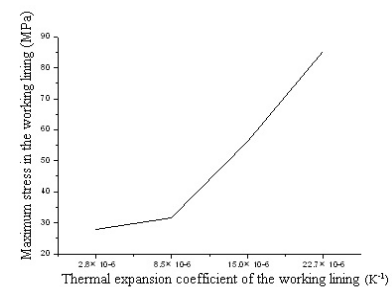


Figure 12 Variation of the maximum stress in the working lining.

Fig.12 illustrated the maximum stress profile of the working lining on the basis of thermal expansion coefficient of the working lining made of alumina-magnesia-carbon material increased from $2.8 \times 10^{-6} \text{ K}^{-1}$ into $22.7 \times 10^{-6} \text{ K}^{-1}$. Note that thermal expansion coefficient of the working lining made of alumina-magnesia-carbon material was less than $15.0 \times 10^{-6} \text{ K}^{-1}$ as to the maximum stress of the working lining made of alumina-magnesia-carbon material within its crushing strength 56.2MPa.

Fig.13 demonstrated the maximum equivalent stress profile of the working lining on the basis of Young's modulus of the working lining made of alumina-magnesia-carbon material expanded from 1GPa into 15GPa. Young's modulus of the working lining made of alumina-magnesia-carbon material was less than 11GPa as to the maximum stress of the working lining made of alumina-magnesia-carbon material within its crushing strength 56.2MPa.

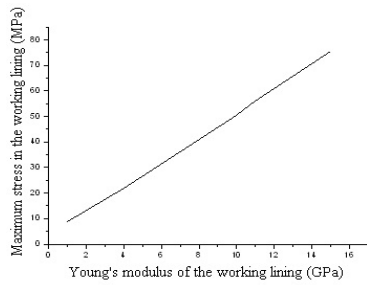


Figure 13 Maximum stress variation in the working lining.

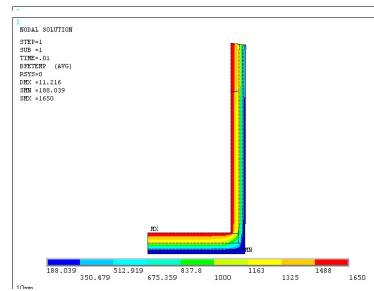


Figure 15 Equivalent temperature with 10mm working lining thinning.

4.5. Working-lining Thickness Influencing Temperature and Stress Field

The working-lining thickness directly affected temperature field distribution of the ladle, so it also affected stress field distribution of the ladle. As the working lining was subjected to erosion of molten steel, steel slag and high-temperature surroundings on it, it became thicker. Accordingly, temperature in the ladle lining and outer shell arising led to change of the ladle stress. In order to research the effect of the working lining thickness on the ladle temperature field and stress field during the process of receiving molten steel, here, on the basis of original thickness 170mm of the working layer of the ladle wall and original 230mm of the working layer of the ladle bottom, they were thinned by 0mm, 10mm and 20mm, but thickness of the working layer and ladle thickness was unaltered. Equivalent temperature and stress contours of thinning by 0mm, 10mm and 20mm were attained through analysis and calculation, respectively, which were shown as Fig.14-19.

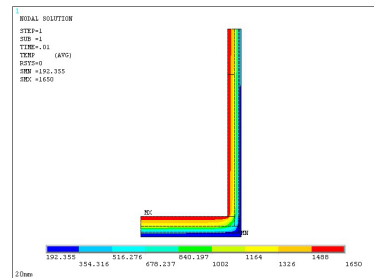


Figure 16 Equivalent temperature with 20mm working lining thinning.

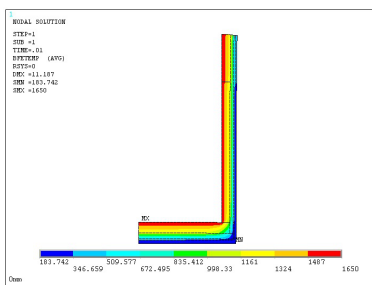


Figure 14 Equivalent temperature with 0mm working lining thinning.

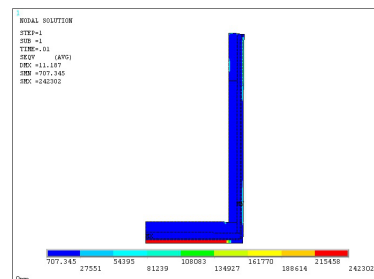


Figure 17 Equivalent stress with 0mm working lining thinning.

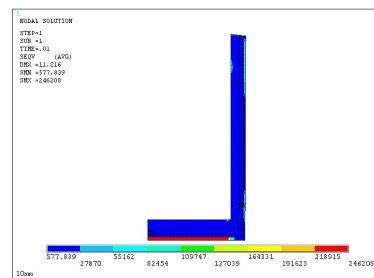


Figure 18 Equivalent stress with 10mm working lining thinning.

From Fig.14-Fig.16, on the basis of other conditions kept, thickness of working lining material of the ladle is only altered and the decrease is from 0mm to 20mm. Temperature distribution laws are uniform basically. The hot

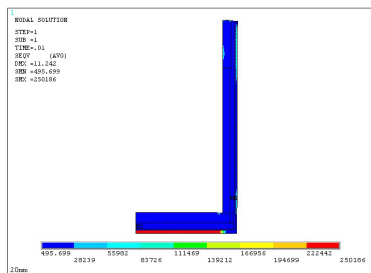


Figure 19 Equivalent stress with 20mm working lining thinning.

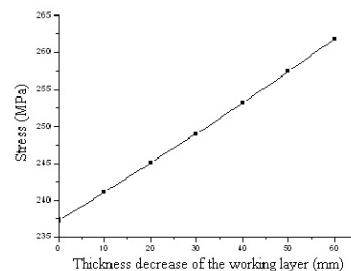


Figure 21 Equivalent stress of a point on the ladle shell bottom.

surface temperature of the working lining is 1650°C. The lowest temperature of the shell is 183.7°C, 188°C and 192.4°C, respectively. Temperature at other locations arises; From Fig.17-Fig.19, laws of equivalent stress distribution were identical basically. The maximum stress (on the outer shell) is 242.3MPa, 246.2MPa and 250.2MPa, respectively.

In order to understanding ladle temperature and stress field with different working lining thickness, thickness of both the ladle wall and bottom was diminished by 60mm based on the working-lining original thickness. The diminishing interval was 10mm. A point on the ladle-shell bottom was taken as an example, whose equivalent stress with change of the working lining thickness was shown as Fig.20 and Fig.21.

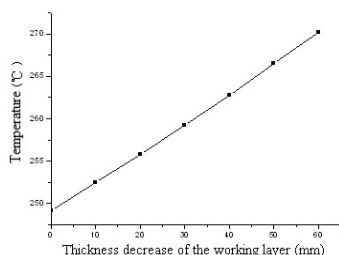


Figure 20 Temperature of a point on the ladle shell bottom.

From Fig.20 and Fig.21, note that the equivalent stress at a point on the ladle shell bottom enlarged uniformly as the working lining thickness decreased. This illustrated that enlarging working-lining thickness made for reducing stress in the ladle shell, not including the ladle cost; similarly, the working-lining thickness could not diminished too much in order to keep the ladle shell stress within the allowable range. Determining an equivalent point between them played an extraordinarily role in designing a ladle.

5. Conclusions

There were many factors affecting the temperature and stress field in the ladle. In this paper, we have analyzed some major factors, such as thermal conductivity, thermal expansion coefficient, Young's modulus of working-lining material and its thickness. Calculation results indicate that at the premise of other conditions being kept unchanged.

- 1) The larger thermal conductivity, the less the temperature gradient across the working lining and the higher corresponding temperature of the permanent lining and ladle shell. Meanwhile, minor stress is generated because of the temperature gradient. But the strength decreased since material temperature is higher.
- 2) The larger thermal expansion coefficient, the greater the stress induced near the high temperature surface of the working lining.
- 3) The larger Young's modulus, the greater the stress introduced near the high temperature surface of the working lining. However, a material with greater Young's modulus and thermal conductivity coefficient is available to a larger strength. Therefore, an equilibrium point between the high stress and great strength is ascertained to restrict the stress induced near the high temperature surface of the working lining to one which is less than the allowable material strength.
- 4) The ladle temperature and stress increase as thickness of working lining material of the ladle decreases.

The lining erosion became more and more serious, which led to increment of the ladle stress and reduction of service life of the ladle as application times of the ladle increased. The actual operation result indicates that the research increases the ladle lifetime effectively and shows its wide popularization value.

Acknowledgement

This research reported in the paper is supported by Natural Science Foundation of Hubei Province of China (2010CDA023), National Natural Science Foundation of China (51075310) and The Hubei Province Key Laboratory of Refractories and Ceramics Ministry-Province jointly-Constructed Cultivation Base for State key Laboratory (G201007). This support is greatly acknowledged.

References

- [1] G.Z Jiang, J.Y Kong and G.F Li, Energy for Metallurgical Industry **41**, 25 (2006).
- [2] G.Z Jiang, J.Y Kong and G.F Li, China Metallurgy **30**, 16 (2006).
- [3] G.F Li, G.Z Jiang and J.Y Kong, Machinery Design and Manufacture **113**, 1 (2010).
- [4] G.S Sarmirtoc, UNITECR **327**, 27(2002).
- [5] J.Y Kong, N Li and Y.R Li, Journal of Hubei Institute of Technology **6**,17 (2002).
- [6] G.Z Jiang, J.Y Kong and G.F Li, China Metallurgy **25**, 17 (2007).
- [7] Z.G Wang, N Li and J.Y Kong, Metallurgy and Energy **30**, 16(2006).
- [8] X.H Xu, W.P Ye, Application of computers in material science, Beijing: China machine press, 2003.
- [9] L.W Millet, Iron and Steel Engineer **58**,63 (1986).
- [10] G.F Li, G.Z Jiang and J.Y Kong, Machinery Design and Manufacture **221**, 1 (2010).



Gongfa Li received the Ph.D. degree in mechanical design and theory from Wuhan University of Science and Technology in China. Currently, he is an associate professor at Wuhan University of Science and Technology, China. His major research interests include modeling and optimal control of com-

plex industrial process. He is invited as a reviewer by the editors of some international journals, such as Environmental Engineering and Management Journal, International Journal of Engineering and Technology, International Journal of Physical Sciences, International Journal of Water Resources and Environmental Engineering, etc. He has published nearly ten papers in related journals.



Peixin Qu was born in 1977. He is a lecturer of Henan institute of science and technology, and received his M.S. degree in radio physics department of physical electronics from Belarusian State University in 2007. His current research focuses on embedded systems applications and embedded security research.



Jianyi Kong received the Ph.D. degree in mechanical design from Universit?t der Bundeswehr Hamburg, Germany, in 1995. He was awarded as a professor of Wuhan University of Science and Technology in 1998. Currently, he is the president of Wuhan University of Science and Technology, China. He services on

the editorial boards of the Chinese journal of equipment manufacturing technology. He is a director of the Chinese society for metals, etc. His research interests focus on intelligent machine and controlled mechanism, dynamic design and fault diagnosis in electromechanical systems, mechanical CAD/CAE, intelligent design and control, etc.



Guozhang Jiang was born in Hubei province, P. R. China, in 1965. He received the B.S. degree in Changan University, China, in 1986, and M.S. degree in Wuhan University of Technology, China, in 1992. He received the Ph.D. degree in mechanical design and theory from Wuhan University of Science and Technology, China, in 2007.

He is a Professor of Industrial Engineering, and the Assistant Dean of the college of machinery and automation, Wuhan University of Science and Technology. Currently, his research interests are computer aided engineering, mechanical CAD/CAE and industrial engineering and management system.



Liangxi Xie is an associate professor in Wuhan University of Science and Technology, China. He major in mechanical design and theory and focus on the research of rotary vane steering gear (RVSG) and vane seals. He has published more than ten papers in related journals.



Zehao Wu was born in Hubei province, P. R. China, in 1987. He received M.S. degree in mechanical engineering and automation from Wuhan University of Science and Technology, Wuhan, China, in 2006. He is currently occupied in his B.S. degree in mechanical design and theory at Wuhan University of Science and Tech-

nology. His current research interests include mechanical CAD/CAE, signal analysis and processing.



Po Gao was born in Hebei province, P. R. China, in 1985. He received M.S. degree in mechanical engineering and automation from Wuhan University of Science and Technology, Wuhan, China, in 2006. He is currently occupied in his B.S. degree in mechanical design and theory at Wuhan University of Science and Tech-

nology. His current research interests include System modeling and simulation, signal analysis and processing.



Yuan He was born in Sichuan province, P. R. China, in 1988. He received M.S. degree in mechanical engineering and automation from Wuhan University of Science and Technology, Wuhan, China, in 2006. He is currently occupied in his B.S. degree in mechanical design and theory at Wuhan University of Science and Technology. His

current research interests in mechanical and electrical control.